Electronic Supplementary Material (ESI) for Nanoscale.

Supporting Information

Simple Fabrication of Layered Halide Perovskite Platelets and Enhanced Photoluminescence from Mechanically Exfoliated Flakes

Balaji Dhanabalan[†¥], Andrea Castelli[†], Milan Palei[≠], Davide Spirito[≠], Liberato Manna[†], Roman Krahne[≠], and Milena Arciniegas[†]**

[†]Nanochemistry Department, [≠]Optoelectronics Group. Istituto Italiano di Tecnologia, Via Morego 30, 16163 Genova, Italy.

[¥]Dipartimento di Chimica e Chimica Industriale, Università degli Studi di Genova, Via Dodecaneso, 31, 16146, Genova, Italy

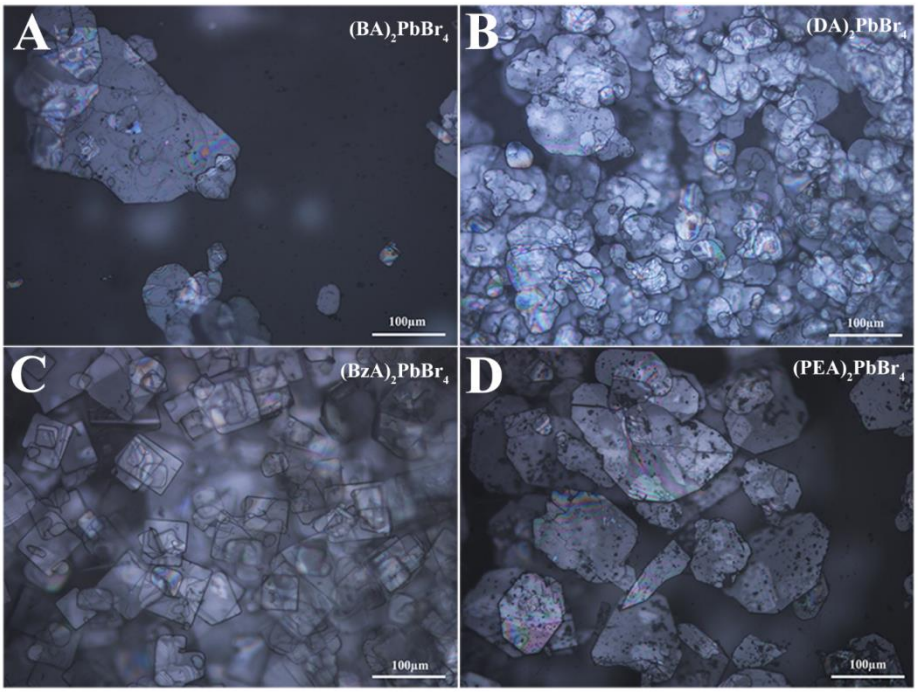

Figure S1. (a-d) Optical microscopy images of the as-synthesized ensembles of layered perovskite platelets prepared with BA (a), DA (b), BzA (c), and PEA (d) amines. Lateral size of a few hundred micrometers are observed from BA-, BzA- and PEA-based crystals, whereas, the lateral size of the crystals prepared with longer chain amine (Da) are reduced to few micrometers.

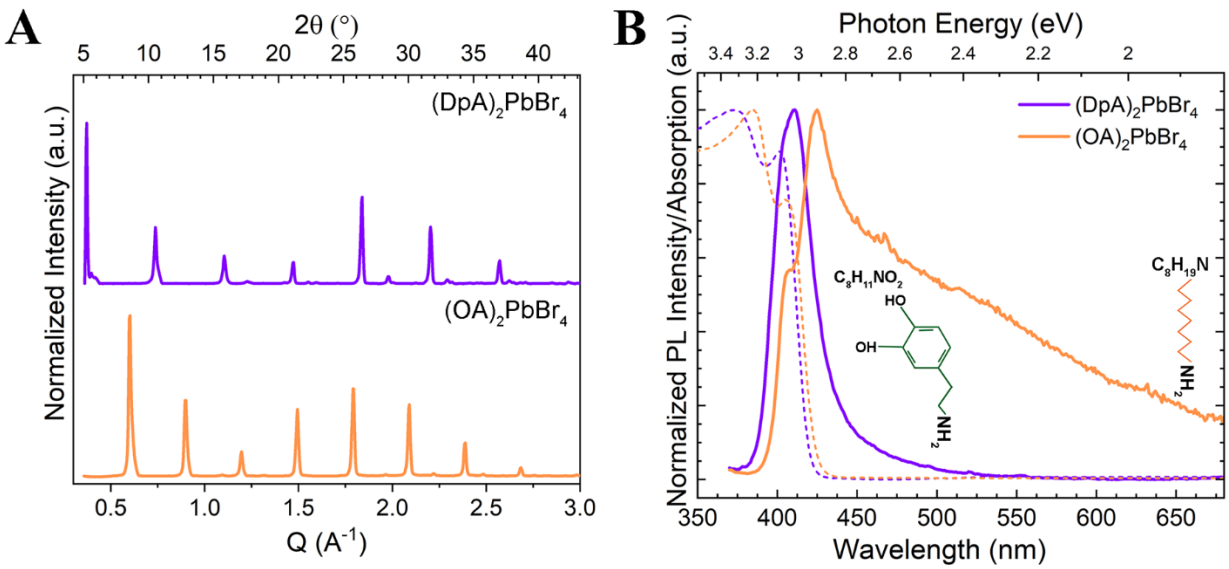

Figure S2. (a) X-ray diffraction patterns collected from the as-synthesized crystals prepared from octylamine (orange) and dopamine (violet) showing periodic diffraction peaks associated to *d* values of 21.11 ± 0.14 Å and 17.14 ± 0.06 Å for octylammonium (OA) and dopammonium (DpA), respectively. (b) Absorbance (dotted lines) and photoluminescence (solid lines) spectra of the $(OA)_2PbBr_4$ and $(DpA)_2PbBr_4$ ensembles.

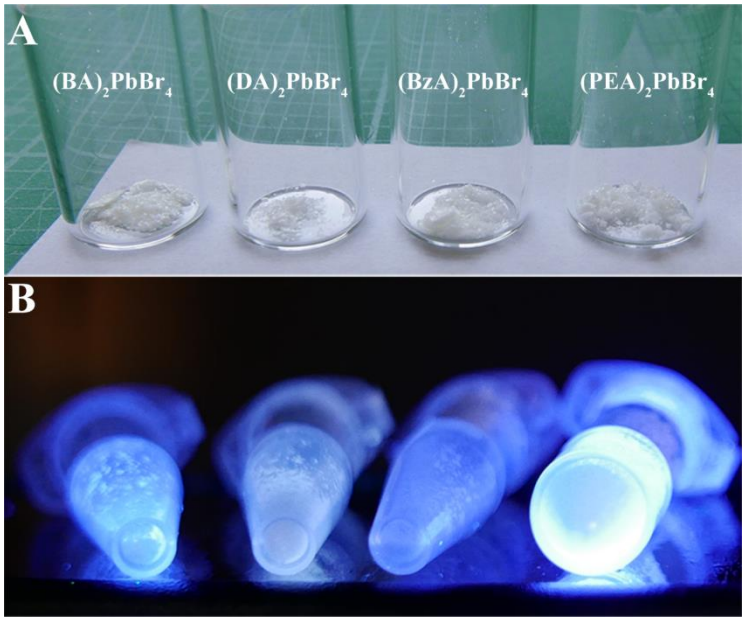

Figure S3. Photographs of the dried layered perovskite ensembles of platelets prepared with different organic spacers taken under normal (a) and ultra-violet (UV) light (b). All the crystals show a bluish-white emission under UV light.

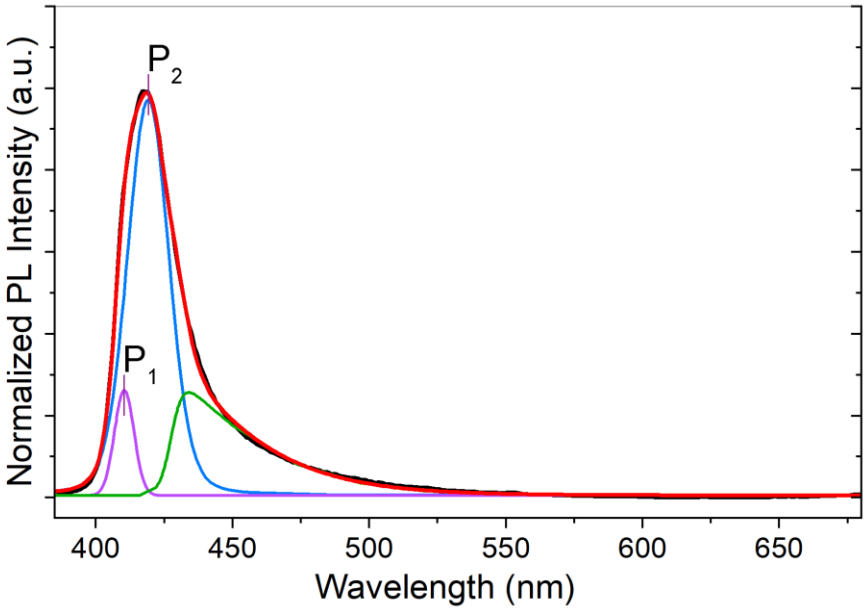

Figure S4. Photoluminescence spectrum acquired from the $(BzA)_2PbBr_4$ crystals showing the sum of functions needed to fit well the profile: a Gaussian (in violet) and a Voigt (in blue) functions for the excitonic distribution, with an additional asymmetric double sigmoidal function for the PL tail. This analysis indicates the presence of two excitonic states with peak maxima at 410 nm (P_1) and 419 nm (P_2).

Table S1. Fitting parameters of the PL time decay curves acquired at the high and low emission peaks, P_1 and P_2, observed in the photoluminescence spectra for each type of crystal and presented in Fig. 3 of the main text for P_1. No significant differences were found between the PL decay time recorded at the different emission peaks.

Crystals		**τ_1, ns**	**A1**	**τ_2, ns**	**A2**	**τ_3, ns**	**A3**	**τ_{Avg}, ns**	**PLQY, %**
BA-	P_1	1.59 ± 0.04	0.41	3.94 ± 0.04	0.52	12 ± 0	0.07	5.43	8±1
	P_2	1.22 ± 0.05	0.27	3.85 ± 0.09	0.68	11.67 ± 0.53	0.09	5.78	
DA-	P_1	1.86 ± 0	0.65	4.04 ± 0	0.30	5.29 ± 0	0.12	3.44	<2
	P_2	1.97 ± 0	0.71	4.76 ± 0	0.29	1.98 ± 0	0.06	3.30	
BzA-	P_1	0.95 ± 0.01	1.06	4.50 ± 0	0.08	5.37 ± 0.59	0.04	2.33	<2
	P_2	0.95 ± 0	0.99	4.41 ± 0.12	0.14	13 ± 0	0.008	3.00	
PEA-	P_1	1.24 ± 0.05	0.15	5.35 ± 0.1	0.64	14.11 ± 0.36	0.22	9.24	15±1.5
	P_2	1.25 ± 0	0.11	5.63 ± 0.11	0.67	14.66 ± 0.39	0.23	9.68	

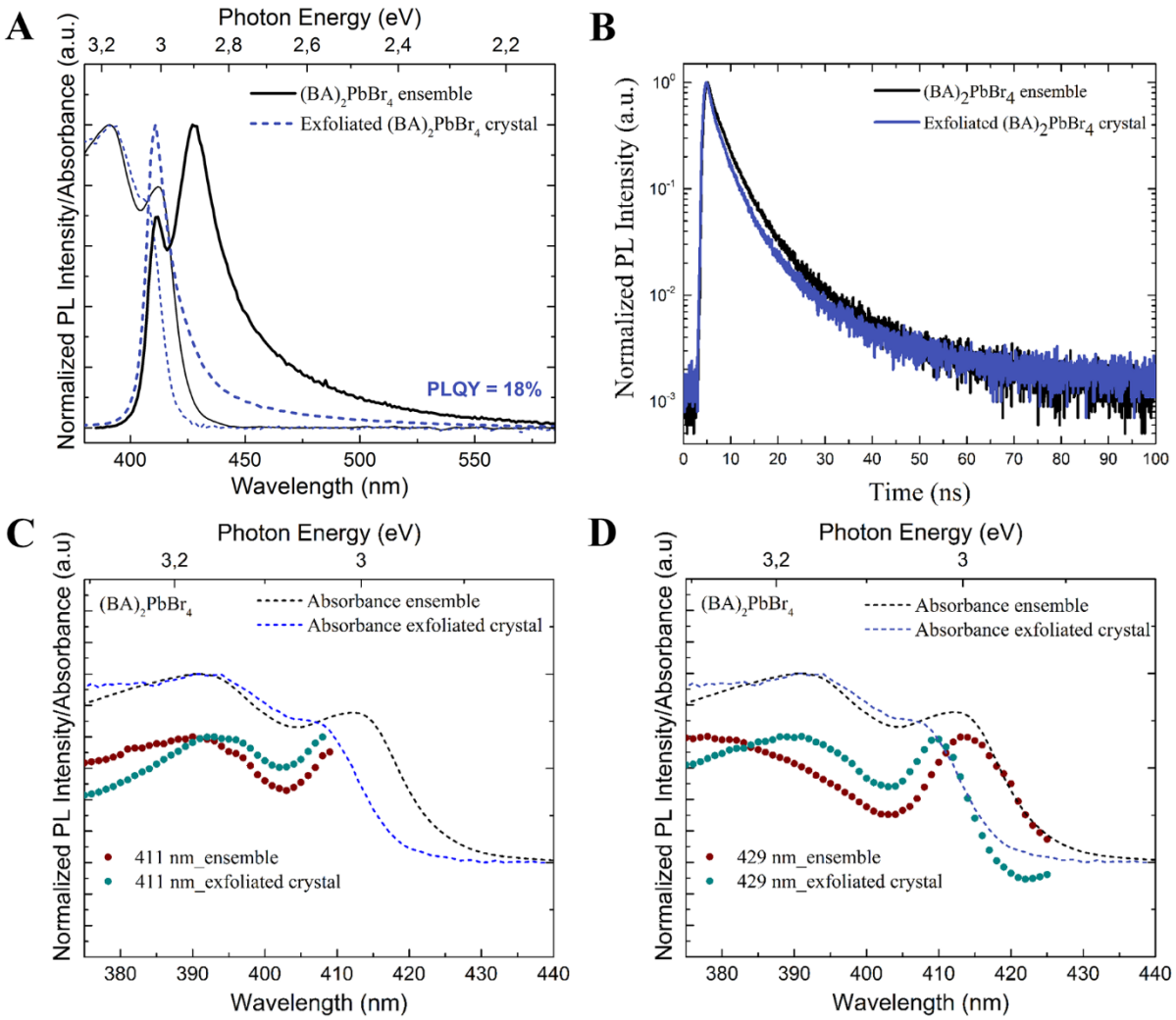

Figure S5. Optoelectronic properties of ensemble and exfoliated $(BA)_2PbBr_4$ crystals. (a) Normalized PL and absorbance spectra acquired before and after exfoliation. Exfoliated crystals show a sharp and single emission peak compared to those collected from their ensembles. The PLQY value is enhanced from 8% to 18 % for the exfoliated crystals. (b) Normalized PL intensities as a function of the decay times before and after exfoliation. (c-d) PL excitation spectra acquired from ensemble and exfoliated crystals recorded at 412 nm (c) and 429 nm (d).

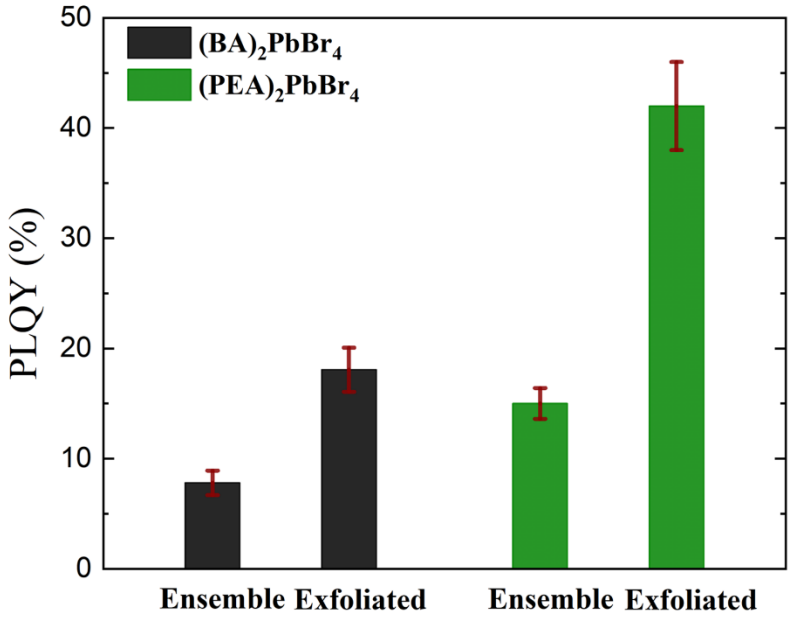

Figure S6. Average PLQY values measured from the selected crystals before and after exfoliation; the statistical errors are shown by the vertical bars. The PLQY values for exfoliated samples are much higher than those obtained from the ensembles.

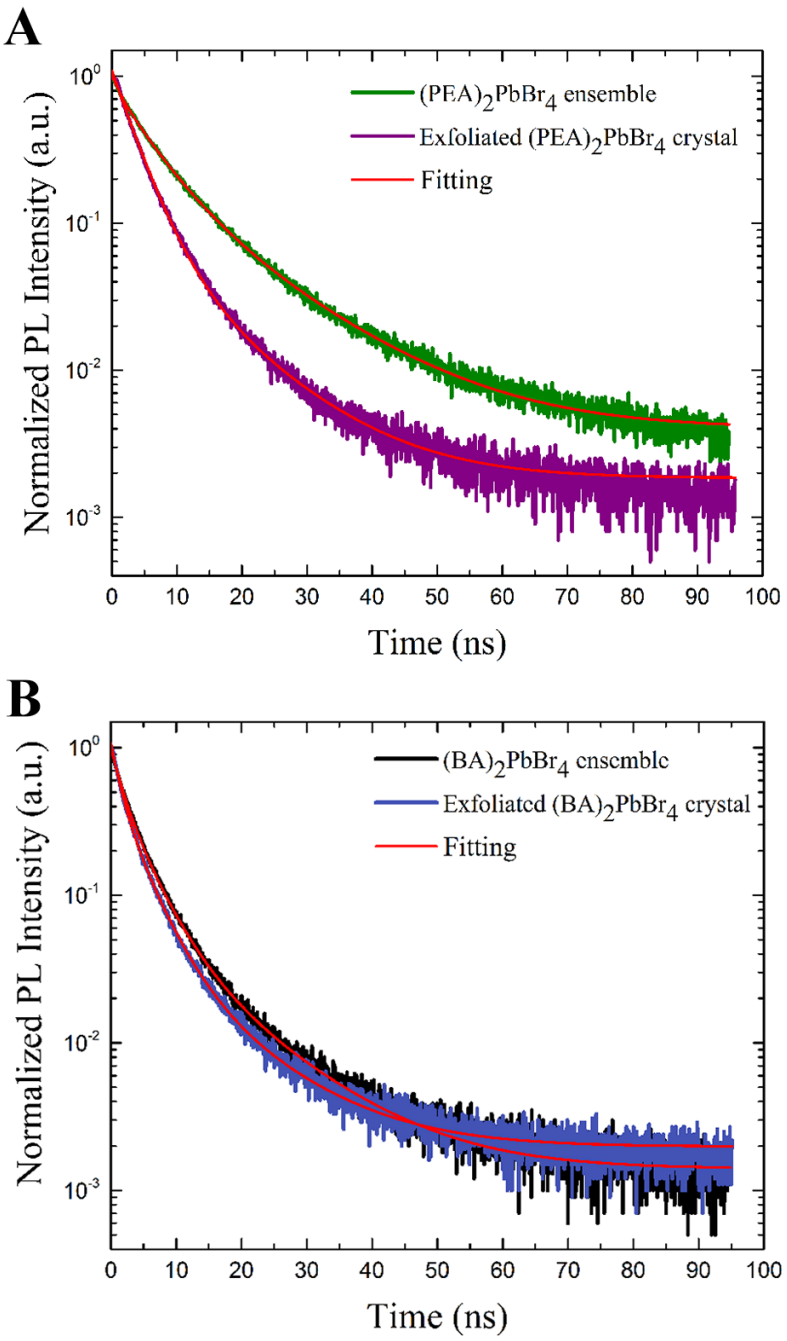

Figure S7. Curve-fitting of the time-correlated single-photon counting (TCSPC) measurements. A three-exponential decay function was employed to fit the decay traces.

Table S2. Optical features of the $(BA)_2PbBr_4$ and $(PEA)_2PbBr_4$ ensembles (A) and exfoliated crystals (E).

Sample	Absorption peaks, nm (eV)		Emission peaks, nm (eV)	
	P_1	P_2	P_1	P_2
$(BA)_2PbBr_4$ A	392 (3.16)	412 (3.01)	411 (3.02)	429 (2.89)
$(BA)_2PbBr_4$ E	392 (3.16)	407 (3.05)	411 (3.02)	-
$(PEA)_2PbBr_4$ A	396 (3.13)	414 (3.00)	412 (3.01)	426 (2.91)
$(PEA)_2PbBr_4$ E	396 (3.13)	407 (3.05)	412 (3.01)	-

Table S3. Fitting parameters of the PL time decay curves presented in Fig. S4 and Fig. 5 of the main text for the ensembles (A) and exfoliated (E) crystals of $(BA)_2PbBr_4$ and $(PEA)_2PbBr_4$ for the emission peaks (P_1 and P_2) observed in their photoluminescence spectra and reported in Table 1. τ_1, τ_2 τ_3, and τ_{Avg} are the three-exponential time decay fitting and their average value. The last column shows the PLQY of the selected layered perovskite before and after exfoliation.

Crystal		τ_1, ns	A1	τ_2, ns	A2	τ_3, ns	A3	τ_{Avg}, ns	PLQY, %
BA-A	P_1	1.59 ± 0.04	0.41	3.94 ± 0.04	0.52	12.00 ± 0	0.07	5.43	8±1
	P_2	1.22 ± 0.05	0.27	3.85 ± 0.09	0.68	11.67 ± 0.53	0.09	5.78	
BA-E	P_1	1.31 ± 0	0.54	3.73 ± 0	0.48	11.44 ± 0	0.05	4.61	18±2
	P_2	1.21 ± 0.02	0.40	3.70± 0.07	0.56	13.00 ± 0.58	0.05	5.41	
PEA-A	P_1	1.24 ± 0.05	0.15	5.35 ± 0.1	0.64	14.11 ± 0.36	0.22	9.24	15±1.5
	P_2	1.25 ± 0	0.11	5.63 ± 0.11	0.67	14.66 ± 0.39	0.23	9.68	
PEA-E	P_1	3.15 ± 0.11	0.07	5.54 ± 2.01	0.94	11.3 ± 0	0.07	5.01	42±4
	P_2	2.89 ± 0.03	0.08	8.08 ± 0.71	0.92	11.3 ± 0	0.07	5.40	

The average lifetime for three exponential decay were calculated using the following relation[1]

$$\tau_{Avg} = \frac{A_1\tau_1^2 + A_2\tau_2^2 + A_3\tau_3^2}{A_1\tau_1 + A_2\tau_2 + A_3\tau_3}$$

Table S4. Analysis of dynamic PL recorded on ensemble and exfoliated $(BA)_2PbBr_4$ and $(PEA)_2PbBr_4$ perovskite crystals. $\boldsymbol{\kappa_r}$, and $\boldsymbol{\kappa_{nr}}$, are the radiative and non-radiative recombination rates, respectively; $\boldsymbol{\kappa_r}$ *Inc.* and $\boldsymbol{\kappa_{nr}}$ *Inc.* represent the calculated percentage increase in $\boldsymbol{\kappa_r}$, and $\boldsymbol{\kappa_{nr}}$, when comparing the exfoliated condition (E) with the ensembles (A) of crystals.

Sample		$\boldsymbol{\kappa_r}$, MHz	$\boldsymbol{\kappa_{nr}}$, MHz	$\boldsymbol{\kappa_r}$, ***Inc.***	$\boldsymbol{\kappa_{nr}}$, ***Inc.***
$(BA)_2PbBr_4$ A	P_1	14.74	169.54	-	-
	P_2	13.84	159.15	-	-
$(BA)_2PbBr_4$ E	P_1	39.05	177.87	165%	5%
	P_2	33.25	151.49	140%	-5%
$(PEA)_2PbBr_4$ A	P_1	16.24	92.01	-	-
	P_2	15.5	87.83	-	-
$(PEA)_2PbBr_4$ E	P_1	83.82	115.75	416%	26%
	P_2	77.84	107.49	402%	22%

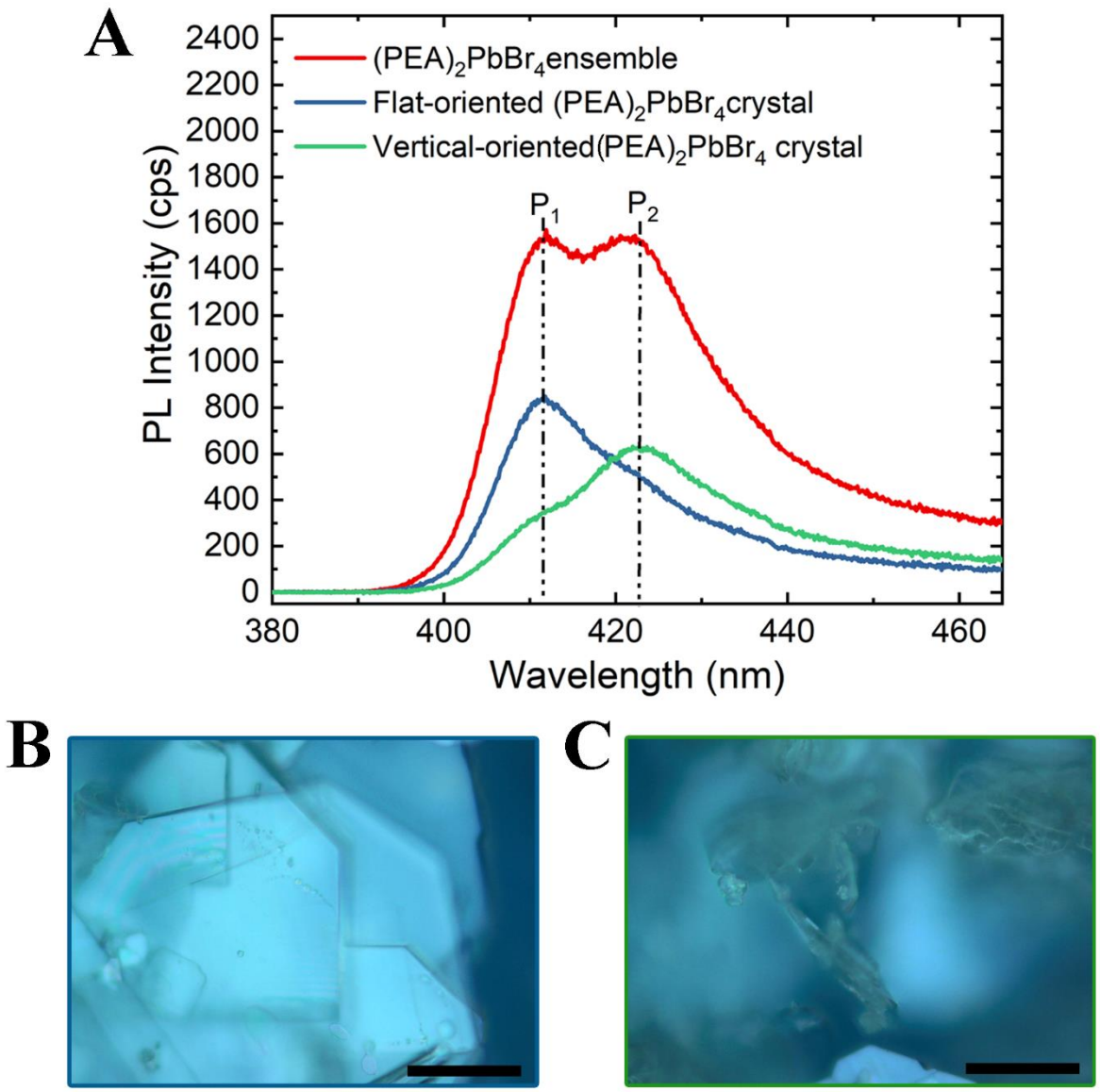

Figure S8. Dependence of the PL spectra on the morphology of the $(PEA)_2PbBr_4$ ensembles. A) Micro PL recorded from regions with different platelet orientation. B-C) Optical microscopy images of the regions with predominantly flat (B) and vertical (C) platelet orientation. Scale bars: 100 µm. The low energy peak (P_2) is more prominent in the spectra from the vertically oriented platelets, while the high energy peak (P_1) is stronger for the flat ensembles.

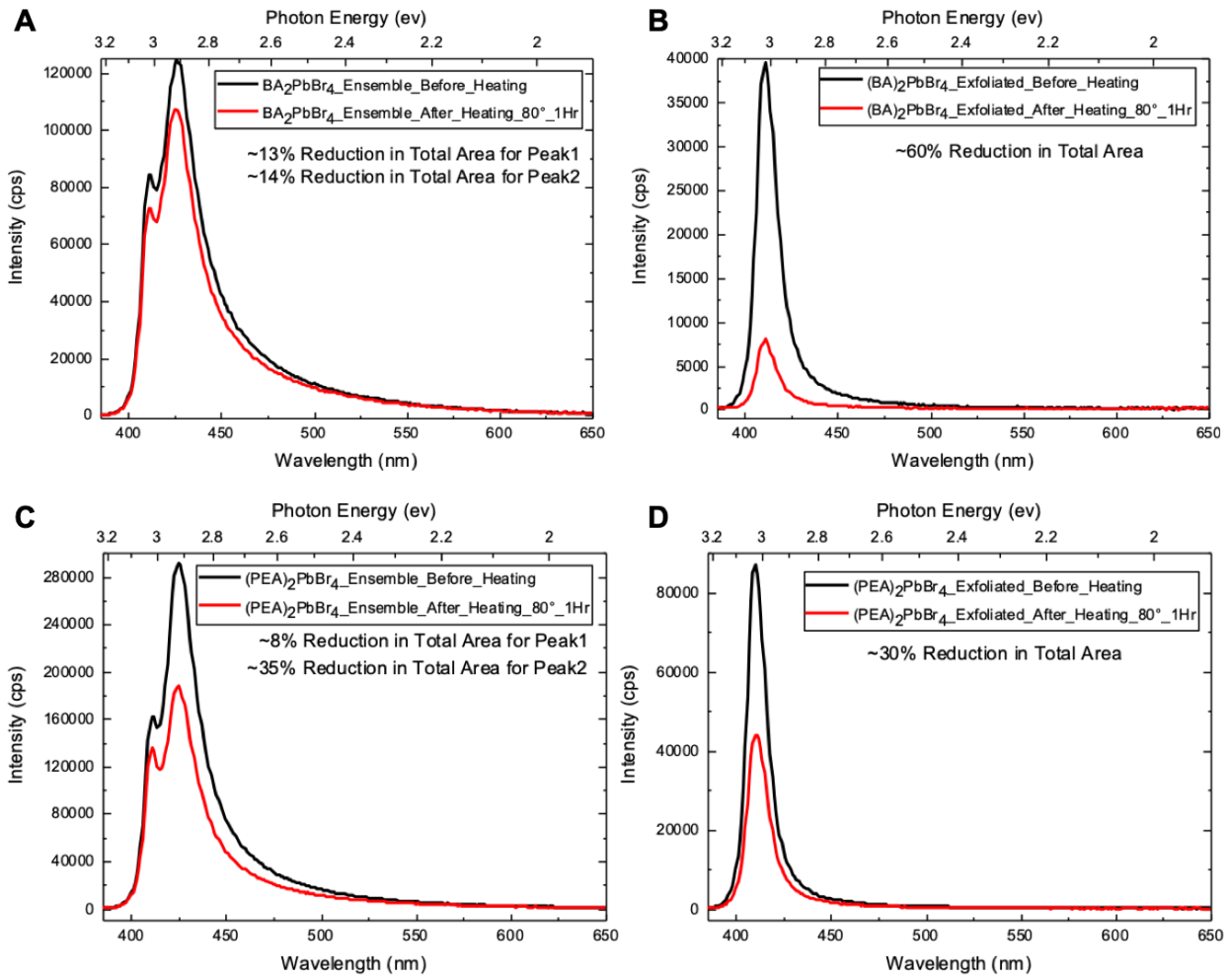

Figure S9. PL spectra recorded before and after heating the samples for 60 minutes at 80°C on a hot plate under ambient conditions. A stronger reduction in the PL intensity is observed for the exfoliated samples (B,D) with respect to the ensembles (A,C), which could be related to the better thermal coupling to the substrate in the case of the exfoliated samples.

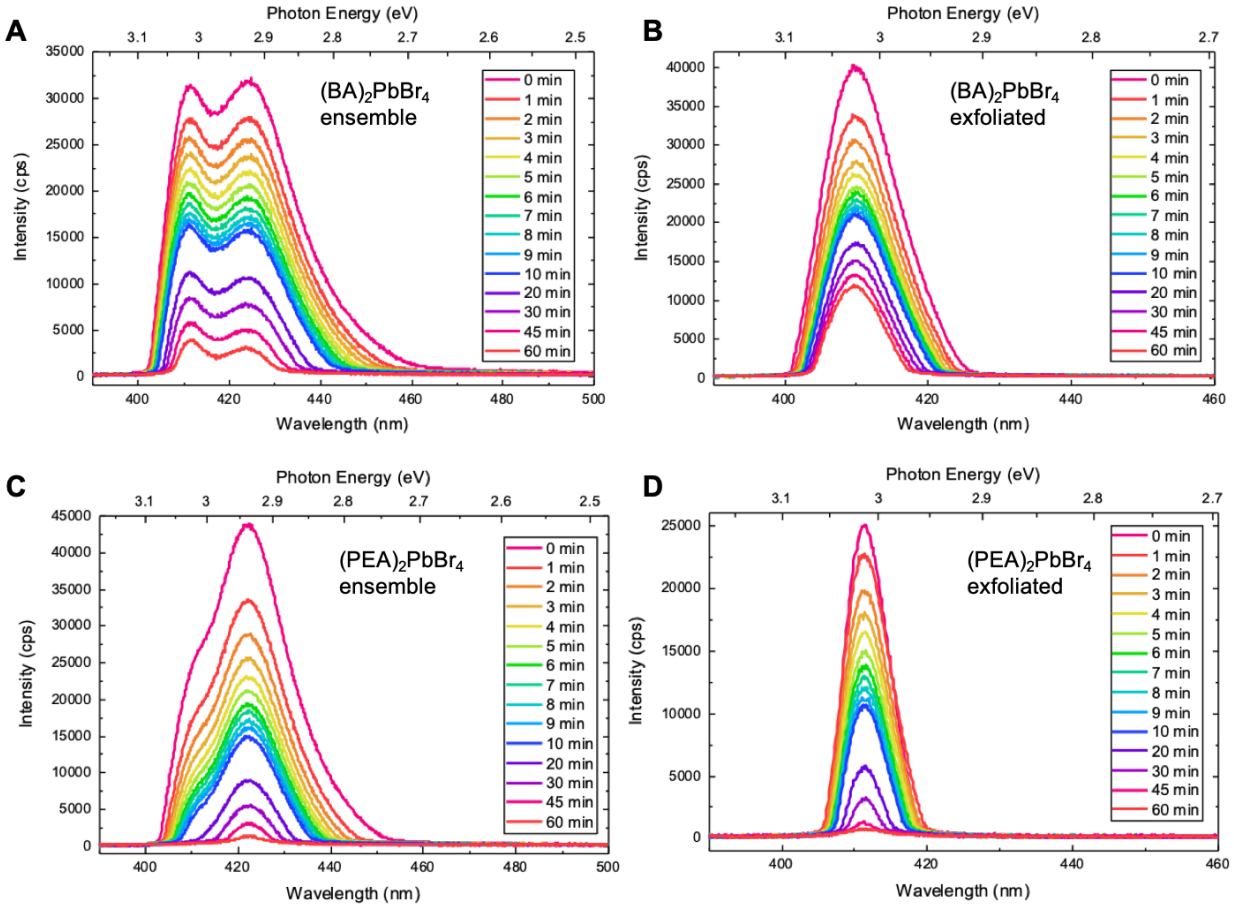

Figure S10. PL spectra of $(BA)_2PbBr_4$ and $(PEA)_2PbBr_4$ ensembles and exfoliated flakes recorded under illumination with a nanosecond pulsed laser at a wavelength of 349 nm (frequency 1 kHz) with an average power density of around 3 mW/cm^2. The PL intensity decreases over time, most likely due to photobleaching.

References

1. Lakowicz, JR, Principles of Fluorescence Spectroscopy. Springer US, New York: 2006.